PHYSICAL REVIEW D **92,** 054025 (2015)

Inclusive weak decays of heavy hadrons with power suppressed terms at NLO

Thomas Mannel, Alexei A. Pivovarov, and Denis Rosenthal
Theoretische Physik 1, Universität Siegen, D-57068 Siegen, Germany
(Received 27 July 2015; published 22 September 2015)

Within the heavy-quark expansion techniques for the heavy hadron weak decays we analytically compute the coefficient of the power-suppressed dimension-five chromo-magnetic operator at next-to-leading order of QCD perturbation theory with the full dependence on the final-state quark mass. We present explicit expressions for the total width of inclusive semileptonic decays including the power-suppressed terms and for a few moments of decay differential distributions. One of the important phenomenological applications of our results is a precision analysis of the decays of bottom mesons to charmed final states and the extraction of the numerical value for the Cabibbo-Kobayashi-Maskawa matrix entry $|V_{cb}|$.

DOI: 10.1103/PhysRevD.92.054025 PACS numbers: 13.20.He, 12.38.Bx, 12.38.-t, 12.39.Hg

I. INTRODUCTION

Presently the Standard Model (SM) of fundamental interactions is being thoroughly tested experimentally at colliders, but no definite signs of new physics have been detected beyond the framework of the Standard Model. New particles have not been explicitly seen and no significant deviations from the Standard Model values in the loop-sensitive Wilson coefficients for flavor-changing observables have been determined in high precision data (for a review, see e.g. Ref. [1]). Thus, the Standard Model has successfully passed all tests in the areas where it is certainly valid as a low-energy effective theory.

However, there is definitely life beyond the SM. Some new phenomena—like neutrino masses and mixing—can be readily incorporated in a rather straightforward manner as simple extensions of the SM. The other new effects like dark matter and dark energy are of cosmological nature; they are related to the still poorly understood realm of gravity and thus are, strictly speaking, outside the particle physics described by the SM. Nevertheless, it seems certain that the scale of the traditionally expected extensions of the Standard Model—like supersymmetry or extra dimensions—has definitely moved from the few-TeV region to a higher one at energies that can make it unreachable at accelerators in the foreseeable future (e.g. [2]). Since the new physics scale has moved higher, the direct observation of new physics phenomena will probably not be explicit even at new machines, although one still has to wait for the results of the 14 TeV run of the LHC. In the case that nothing is seen, any new phenomena beyond the Standard Model can only be identified through detecting slight discrepancies between theoretical predictions within the SM and precision measurements at low energy with available tools.

Accurate theoretical predictions within the SM are of crucial importance in such a scenario. For these predictions to be reliable one first needs the precise numerical values for the key parameters of the SM itself. The least precisely known sector of the SM is the quark flavor one where the quark Yukawa couplings to the Higgs field are not well known numerically. In the Standard Model they translate into the mixing angles between generations gathered in the Cabibbo-Kobayashi-Maskawa (CKM) matrix and the vacuum expectation value of the Higgs field. The latter can be determined from the leptonic sector. Note that the flavor sector is also a most promising place for investigating the Higgs mechanism that is definitely of an effective origin and probably will be modified in the future as the presence of a fundamental scalar in the "final" theory does not look convincing. All in all, the flavor physics of quarks is a promising place to search for new physics and should be thoroughly studied (see, e.g. Refs. [3,4]).

While the quark weak decays are mediated by the charged weak currents at tree level, which are believed not to have sizable contributions of possible new physics, their study is of importance for the precise determination of the numerical values of the CKM matrix elements. However, obtaining solid theoretical predictions for processes with quarks at the fundamental level requires the use of genuinely nonperturbative computational methods like QCD lattice calculations since eventually one has to make a prediction for the experimental quantities that include hadrons and cannot be described in the perturbation theory of QCD due to confinement. This is the principal part of the problem, but there is also a purely technical part. Even if the direct computation in terms of quarks would be relevant to the world of hadrons (this partly can be made possible by choosing proper observables) one will still face the problem of the computational complexity of the calculation with sufficient accuracy that requires a rather large order of perturbation theory. An example is the description of the process $b \to s\gamma$.

In inclusive processes the partonic decay rate is known to be the leading term of an expansion in inverse powers of the heavy-quark mass. At that level, the computation of hadronic processes is technically equivalent to just taking the parton level of the computation for hadronic processes. This fact makes the technical part equivalent to that of the leptonic calculations where the benchmark level for the up-to-date technology of the computation is the evaluation of the muon lifetime. The muon decay is a source for the determination of the Fermi constant G_F with high accuracy from a leptonic sector. The first radiative corrections were computed a long time ago [5,6]. To match the precision of the present experimental data for the muon lifetime, the theoretical calculations have to be performed with very high accuracy. In this case the calculations are very precise, since the purely leptonic decays are well described within perturbation theory and the expansion parameter $\alpha \approx 1/137$ is small. The latest theoretical result includes the next-to-next-to-leading order (NNLO) radiative corrections in the fine-structure constant expansion [7]

$$\Gamma(\mu \to \nu_\mu e \bar{\nu}_e) = \frac{G_F^2 m_\mu^5}{192\pi^3}\left\{1 + \left(\frac{25}{8} - \frac{\pi^2}{2}\right)\frac{\alpha_r}{\pi} + (6.743 + \Delta\Gamma^{had})\left(\frac{\alpha_r}{\pi}\right)^2\right\}. \quad (1)$$

Here m_μ is the muon mass. The numerical value for the electron mass m_e is set to zero everywhere but in the expression for the expansion parameter

$$\alpha_r = \alpha + \frac{2\alpha^2}{3\pi}\ln\frac{m_\mu}{m_e}.$$

The expressions that account for a nonvanishing electron mass are known. The quantity $\Delta\Gamma^{\rm had} = -0.042 \pm 0.002$ is the hadronic contribution that is known with an uncertainty of about 5%. It cannot be computed from first principles for light quarks and is obtained by integrating the experimental data for the photon vacuum polarization. Note that a similar situation emerges with the precision analysis of one of the key leptonic observables—the muon anomalous magnetic moment $g-2$. At present the hadronic contributions related to light quarks give the main uncertainty of the theoretical prediction (e.g. [8,9]). It is a general feature that the quark sector influences even pure leptonic processes if the required accuracy is high enough (e.g. [10]).

Equation (1) results in an $\mathcal{O}(1\ \text{ppm})$ accuracy of the theoretical expression for the lifetime such that its precision is comparable with that of modern experimental data. As far as the quark sector is concerned, there is a good set of data for $s \to u$ weak transitions that corresponds to $K \to \pi e \bar{\nu}_e$ decays at the hadron level, but it is hopeless to precisely compute the related rate theoretically at present because of strong infrared problems in the theoretical treatment of reactions with light hadrons.

For heavy hadrons the theoretical treatment of the decays is however possible because the large mass of the heavy quark constitutes a perturbative scale that is much larger than $\Lambda_{\rm QCD}$. The leading logarithmic effects related to that scale were discussed long ago [11]. Later a framework was created for the possibility for an expansion in powers of $\Lambda_{\rm QCD}/m_Q$ where m_Q is the quark mass and $\Lambda_{\rm QCD} \sim 500$ MeV is a typical hadronic scale [12–14]. Top quarks do not form mesons due to their short lifetime, and charmed mesons are probably not heavy enough, rendering the convergence of an expansion in the inverse mass marginal, but the case of bottom-meson decays is certainly tractable in this way and thus has been intensively studied. The technique is applicable to the $b \to u$ and $b \to c$ transitions and both to semileptonic and purely hadronic inclusive decays. For definiteness, we will stick to semileptonic $b \to c$ decays.

Subleading terms in this combined expansion in $\Lambda_{\rm QCD}/m_Q$ and $\alpha_s(m_Q)$ have been investigated in some detail, in particular, for the inclusive semileptonic case. The tree-level terms are known up to $(\Lambda_{\rm QCD}/m_Q)^5$ [15], while the leading term in $\Lambda_{\rm QCD}/m_Q$, i.e. the partonic rate is known to NNLO accuracy [16,17]. More recently, the corrections of order $\alpha_s(m_Q)(\Lambda_{\rm QCD}/m_Q)^2$ have been investigated. The contribution $\alpha_s(m_Q)\mu_\pi^2/m_Q^2$ is linked to the leading-order one through the reparametrization invariance [18] (see, the explicit calculation in Ref. [19]) while the next-to-leading-order (NLO) corrections to the chromomagnetic operator contribution require an independent calculation.

This calculation was performed first in Ref. [20] for the triply differential rate; in order to obtain the total rate or moments a numerical integration needs to be performed, which is subtle due to cancellations of infrared divergences from different contributions. Nevertheless these results have recently been implemented in the extraction of V_{cb} showing that the impact on V_{cb} is of the expected size.

In the present paper we perform a fully analytical calculation of the total rate and selected moments of the coefficient of the chromomagnetic operator at next-to-leading order of QCD perturbation theory with the full dependence on the final-state quark mass. The results of the analogous computation in the massless limit for the final-state quark have been presented earlier in Ref. [21]. Here we present explicit expressions for the total width of inclusive semileptonic decays and for a few moments of differential distributions with full dependence on the final-state quark mass.

The paper is organized as follows. In the next section we give a general representation for the decay width of a heavy hadron in a form suitable for computation in QCD. In Sec. III we give the necessary basics of heavy-quark effective theory (HQET) which is a working tool for the

present calculation. In Sec. IV we write down the heavy-quark expansion (HQE) for the decay rate. The actual computation and results are described in Sec. V. In the Appendixes we give the explicit expressions for our master integrals and some long analytical expressions for the coefficients of the HQE.

II. QCD REPRESENTATION FOR THE DECAY RATE

It is difficult to compute a hadronic decay rate, since the underlying theory of strong interactions—QCD—is formulated in terms of quarks and the hadrons only appear in the strong coupling regime as bound states. Therefore one can either use numerical calculation on the lattice or find special observables for which the perturbation theory calculation is feasible in some form. Such observables are inclusive ones, since the sum over hadronic states can be related to the sum over the quark-gluon states using the unitarity of the theory. In the case when the initial state is treatable in perturbation theory, i.e. it is a leptonic one as in e^+e^- annihilation into hadrons or hadronic τ-lepton decays the results can be uniquely obtained in perturbation theory. In cases when the initial state is hadronic, i.e. it is not tractable in perturbation theory, one uses factorization to separate scales and compute the short-distance effects in perturbation theory while long-distance properties are encoded in hadronic matrix elements. The famous example of the latter approach is the analysis of deep inelastic scattering (DIS) of leptons on hadrons. The analogue of DIS in heavy-quark physics is the inclusive decay of heavy hadrons. One can use either fully hadronic (nonleptonic) decays or semileptonic ones. The number of experimental observables in inclusive hadronic decays is however limited to basically the total rate of the process. In semileptonic decays the presence of leptons in the final states gives more kinematical flexibility while retaining the rigorous theoretical description of the process.

The low-energy effective Lagrangian $\mathcal{L}_{\rm eff}$ for semileptonic $b \to c$ transitions is the four-fermion interaction

$$\mathcal{L}_{\rm eff} = 2\sqrt{2} G_F V_{cb} (\bar{b}_L \gamma_\mu c_L)(\bar{\nu}_L \gamma^\mu \ell_L) + \text{H.c.} \qquad (2)$$

with left-handed fermion fields. The numerical value for the Fermi constant G_F is determined from purely leptonic weak processes and is known with high precision. The mixing angle V_{cb} is the main interest in decay measurements with hadronic initial states [22]. The precision analysis of such processes is important for both the flavor sector and Higgs mechanism investigations in searches for new physics.

Using the unitarity of the $\mathcal{S}$-matrix, the inclusive decay rate $B \to X_c \ell \bar{\nu}_\ell$ is obtained by taking the absorptive part of the forward matrix element of the transition operator $\mathcal{T}$ [23] which is the second-order term of the perturbation theory expansion in the interaction Lagrangian $\mathcal{L}_{\rm eff}$,

$$\mathcal{T} = i \int dx T\{\mathcal{L}_{\rm eff}(x) \mathcal{L}_{\rm eff}(0)\}. \qquad (3)$$

Note that the transition operator $\mathcal{T}$ is a nonlocal operator composed of the fields. There is not much hope of handling matrix elements of such an operator in QCD, in particular when matrix elements are taken with hadronic states.

The idea of HQE is that when taking a matrix element over a heavy hadron containing a heavy quark with mass $m_Q \gg \Lambda_{\rm QCD}$ the correlator does acquire a large internal scale, m_Q, that enables scale separation. For actual separation of scales one applies the operator product expansion techniques. These ideas are formalized through the notion of effective theories. Within the heavy hadron with momentum p_H and mass M_H a large part of the momentum is due to a pure kinematical contribution of the heavy quark $p_H = m_Q v + \Delta$ with $v = p_H/M_H$ being the velocity of the hadron and Δ is related to the light degrees of freedom and interactions between them and the heavy quark. One can already extract the factor related to the large quark part of the momentum explicitly at the level of field variables when the matrix element over a heavy hadron is taken afterwards. The heavy-quark field can be separated into the quickly oscillating phase and a slowly changing field $h_v(x)$ with a typical momentum of order $\Delta \sim \Lambda_{\rm QCD}$

$$Q(x) \sim e^{-i(m_Q v)x} h_v(x). \qquad (4)$$

The velocity $v = p_H/M_H$ is finite in the limit of infinitely heavy quarks $m_Q \gg \Lambda_{\rm QCD}$. This program is realized within the effective theory for heavy quarks. In order to make the dependence of the decay width on the heavy-quark mass m_Q explicit and to build up an expansion in $\Lambda_{\rm QCD}/m_Q$, one matches the time-ordered product of full QCD operators entering the transition operator $\mathcal{T}$ onto an expansion in terms of HQET [24,25]. Presently the HQE in inclusive semileptonic $b \to c$ transitions provides a level of theoretical precision in the prediction of the total inclusive rate for $B \to X_c \ell \bar{\nu}_\ell$ within two percent. The structure of the HQE is given by [26]

$$\Gamma(B \to X_c \ell \bar{\nu}_\ell) = \Gamma^0 |V_{cb}|^2 \left[a_0 \left(1 + \frac{\mu_\pi^2}{2m_b^2}\right) + a_2 \frac{\mu_G^2}{2m_b^2} + a_3 \frac{\bar{\rho}_3}{m_b^3} + a_4 \frac{\bar{\rho}_4}{m_b^4} + \mathcal{O}\left(\frac{\Lambda_{\rm QCD}^5}{m_b^5}\right)\right]$$

where $\Gamma^0 = G_F^2 m_b^5/(192\pi^3)$ and m_b is the b-quark mass. The precise definition and the proper choice of the most suitable mass parameter for the heavy-quark field has been extensively discussed in the literature. The power-suppressed terms are given by the forward matrix elements of the local operators of growing dimensionality in HQET over the heavy hadron state. Their numerical values are

determined by the corresponding power of the QCD infrared parameter of $\Lambda_{\rm QCD}$. These are nonperturbative quantities either to be computed within some nonperturbative techniques such as lattice QCD or to be fitted to experimental data. The kinetic energy parameter μ_π^2 is given by the nonrelativistic kinetic energy operator of the heavy quark within the heavy hadron. The chromomagnetic parameter μ_G^2 is given by the matrix element of the magnetic dipole operator. These two operators give the leading power-suppressed contribution and have been intensively studied. The higher-order power-suppressed terms are becoming important at present as the experimental data improves. The parameter $\bar{\rho}_3$ describes the contribution of dimension-six operators which are the Darwin term and the spin-orbit interaction. The general parameter $\bar{\rho}_4$ is a contribution of a rather large number of dimension-seven operators [15]. The coefficients a_i are functions of the quark and lepton masses and have a perturbative expansion in the strong coupling constant $\alpha_s(m_b)$. The leading-term coefficient a_0 is known analytically to $\mathcal{O}(\alpha_s^2)$ precision in the massless limit of the final-state quark [27]. At this order the mass corrections have been accounted for analytically for the total width as an expansion in the final fermion mass in Ref. [28] and numerically for the differential distribution in Ref. [29]. The coefficient of the kinetic energy parameter is linked to the coefficient a_0 by Lorentz invariance; see the explicit analysis in Ref. [18]. The NLO correction to the coefficient of the chromomagnetic parameter a_2 has been investigated recently in Ref. [20] where the differential distribution has been computed and the total decay rate has been obtained by a process of numerical integration over the phase space. The α_s correction to the chromomagnetic parameter coefficient a_2 has been analytically computed in Ref. [21] in the massless limit. Here we give the result with full mass dependence in analytical form. Our calculation of the coefficient a_2 is in fact a matching computation between QCD and HQET. For this reason we present some facts about HQET that are relevant for our discussion in the next section.

III. BASICS OF HQET

A heavy quark near its mass shell is described by a field $h_v(x)$ which is a remnant of the whole QCD fermion field $Q(x)$. In fact, it effectively contains only large components of the Dirac bispinor that describes the quark and not the antiquark. One achieves the separation of the components by using the projector $P_+ = (1+\not{v})/2$ where v is the external velocity of the heavy hadron containing the heavy quark. Note that obtaining HQET as the effective theory from QCD is very close in spirit to the well-known procedure of obtaining the nonrelativistic limit of QCD or, earlier, QED. The quark velocity v is fixed in the presence of the heavy hadron by its momentum. Usually the common choice for the velocity is $v = p_H/M_H$. The behavior of the time and space components of the formal Lorentz four-tensors differs in HQET. It is useful to split a four-vector p^μ into longitudinal and transverse parts, namely $p^\mu = v^\mu(vp) + p_\perp^\mu$. The covariant derivative of QCD is $\pi_\mu = i\partial_\mu + g_s A_\mu$ with the splitting $\pi^\mu = v^\mu(v\pi) + \pi_\perp^\mu$.

The quantity h_v is the heavy-quark field entering the HQET Lagrangian [24,25]. The effective Lagrangian of HQET can be obtained in a concise form at tree level by integrating out the P_- part of the heavy quark field H_v, $H_v = P_- H_v$, with the result

$$\mathcal{L}_{\rm HQET} = \bar{h}_v(\pi v)h_v + \bar{h}_v \not{\pi}_\perp \frac{1}{2m + \pi v}\not{\pi}_\perp h_v. \tag{5}$$

Here the first term is just the residual energy of the quark while the second one describes the effects of the removed (integrated out) antiquark. It is nonlocal, but in the limit $m \gg \pi v$ one can expand the second term in a series in the inverse large mass and obtain a local Lagrangian up to a given order in the HQE

$$\mathcal{L}_{\rm HQET} = \bar{h}_v(\pi v)h_v + \bar{h}_v \not{\pi}_\perp \frac{1}{2m}\not{\pi}_\perp \bar{h}_v - \bar{h}_v \not{\pi}_\perp \frac{\pi v}{4m^2}\not{\pi}_\perp h_v. \tag{6}$$

It is inconvenient to have time derivatives in a term that is formally a correction, since then the fields h_v are not correctly canonically normalized. Therefore the redefinition of the fields is used to remove time derivatives up to order $1/m^2$

$$h_v \to \left(1 + \frac{\not{\pi}_\perp \not{\pi}_\perp}{8m^2}\right) h_v. \tag{7}$$

One gets the Lagrangian for the new modes h_v (for which we retain the same notation) in the form

$$\mathcal{L}_{\rm HQET} = \mathcal{O}_v + \frac{1}{2m}(\mathcal{O}_\pi + C_{\rm mag}(\mu)\mathcal{O}_G) + \frac{1}{2m^2}\mathcal{O}_3 + \mathcal{O}\left(\frac{\Lambda_{\rm QCD}^3}{m^3}\right) \tag{8}$$

with

$$C_{\rm mag}(\mu) = 1 + \frac{\alpha_s(\mu)}{2\pi}\left\{C_F + C_A\left(1 + \ln\frac{\mu}{m_b}\right)\right\} \tag{9}$$

being the coefficient of the chromomagnetic operator $\mathcal{O}_G$ including the QCD radiative correction of the order α_s [30]. For new modes h_v the terms of order $O(1/m_b^2)$ in the Lagrangian contain no time derivative [25,31]. In Eq. (8) we introduced the following notation. The quantity $\mathcal{O}_v = \bar{h}_v v\pi h_v$ is the leading power energy operator that is

independent of the heavy-quark mass and spin and gives the famous spin-flavor symmetry of HQET. The quantity $\mathcal{O}_\pi = \bar{h}_v \pi_\perp^2 h_v$ is a kinetic energy operator and $\mathcal{O}_G = \frac{1}{2}\bar{h}_v \sigma_{\mu\nu}[\pi_\perp^\mu, \pi_\perp^\nu] h_v$ is a chromomagnetic operator. They constitute the operators appearing at subleading order. Higher terms are given by the operator $\mathcal{O}_3 = \bar{h}_v[\pi_\perp, [\pi_\perp, \pi v]]h_v$ that can further be converted into a linear combination of the Darwin $\mathcal{O}_D = \bar{h}_v[\pi_\perp^\mu, [\pi_\perp^\mu, \pi v]]h_v$ and spin-orbit term $\mathcal{O}_{SL} = \bar{h}_v \sigma_{\mu\nu}[\pi_\perp^\mu, [\pi_\perp^\nu, \pi v]]h_v$, $\mathcal{O}_3 = c_D \mathcal{O}_D + c_{SL}\mathcal{O}_{SL}$ with coefficients c_D, c_{SL} known at the next-to-leading order of perturbative expansion in the strong coupling constant. The discussion of order $1/m_Q^2$ terms in the HQET Lagrangian is relevant for our computation because of the necessity to precisely fix the definition of the fields h_v entering the HQE.

IV. HQE FOR THE WIDTH CORRELATOR

For further convenience we introduce a normalized transition operator $\tilde{\mathcal{T}}$ through the relation

$$\mathrm{Im}\mathcal{T} = \Gamma^0 |V_{cb}|^2 \tilde{\mathcal{T}}. \tag{10}$$

With the use of HQET, the HQE is simply a matching from QCD to HQET

$$\tilde{\mathcal{T}} = C_0 \mathcal{O}_0 + C_v \frac{\mathcal{O}_v}{m_b} + C_\pi \frac{\mathcal{O}_\pi}{2m_b^2} + C_G \frac{\mathcal{O}_G}{2m_b^2}. \tag{11}$$

The local operators $\mathcal{O}_i$ in the expansion (11) are ordered by their dimensionality $\mathcal{O}_0 = \bar{h}_v h_v$, $\mathcal{O}_v = \bar{h}_v v\pi h_v$, $\mathcal{O}_\pi = \bar{h}_v \pi_\perp^2 h_v$, $\mathcal{O}_G = \bar{h}_v \frac{1}{2}[\pi_\perp, \pi_\perp] h_v$. The coefficients of these operators are obtained by matching the relevant matrix elements between QCD and HQET. Note that after taking a matrix element over the hadronic state (like the B meson) one can use the equations of motion for HQET fields h_v to eliminate the operator $\mathcal{O}_v$. By the same token, there is an operator $\mathcal{O}_5 = \bar{h}_v (v\pi)^2 h_v$ that is of higher order in the large mass expansion after going on shell using the equations of motion of HQET. Thus, the expansion (11) is a matching relation from QCD to HQET with proper operators up to dimension five with the corresponding coefficient functions. The coefficients are independent of external states and so we may use a heavy quark and gluons (on shell) as external states for matching to QCD.

Note that one can use the full QCD fields for the HQE as well. However, the choice of the proper basis of operators is not so straightforward as in HQET. Still it is convenient to choose the local operator $\bar{b}\not{v}b$ defined in full QCD as a leading term of the heavy-quark expansion [32]. Indeed, the current $\bar{b}\gamma_\mu b$ is conserved and its forward matrix element with hadronic states is absolutely normalized. For implementing this setup one needs an expansion (matching) of a full QCD local operator $\bar{b}\not{v}b$ in HQE through HQET operators. The expansion reads [33]

$$\bar{b}\not{v}b = \mathcal{O}_0 - \tilde{C}_\pi \frac{\mathcal{O}_\pi}{2m_b^2} + \tilde{C}_G \frac{\mathcal{O}_G}{2m_b^2} + O(\Lambda_{\mathrm{QCD}}^3/m_b^3) \tag{12}$$

up to the necessary order in the strong coupling α_s. The coefficient of the leading power operator $\mathcal{O}_0$ has no radiative corrections and the kinetic operator has the coefficient related to the leading one due to Lorentz (reparametrization) invariance.

Substituting the expansion (12) into Eq. (11) one obtains after using the equation of motion for the operator $\mathcal{O}_v$ in the forward matrix elements

$$\tilde{\mathcal{T}} = C_0 \left\{ \bar{b}\not{v}b - \frac{\mathcal{O}_\pi}{2m_b^2} \right\} + \{ -C_v C_{\mathrm{mag}}(\mu) + C_G - \tilde{C}_G C_0 \} \frac{\mathcal{O}_G}{2m_b^2}. \tag{13}$$

Note that for phenomenological applications the numerical value for the chromomagnetic moment parameter μ_G^2, related to the forward matrix element of the operator $\mathcal{O}_G$, is usually taken from the mass splitting between the pseudoscalar and vector ground-state mesons. The mass difference of bottom mesons $m_{B^*}^2 - m_B^2 = \Delta m_B^2 = 0.49\ \mathrm{GeV}^2$ is given by

$$\frac{1}{2M_B} C_{\mathrm{mag}}(\mu) \langle B(p_B)|\mathcal{O}_G(\mu)|B(p_B)\rangle = \frac{3}{4}\Delta m_B^2, \tag{14}$$

up to higher-order $1/m_Q$ corrections, where we use the relativistic normalization of states. Therefore the coefficient in front of the renormalization-group-invariant combination $C_{\mathrm{mag}}(\mu)\mathcal{O}_G(\mu)$ can be defined independently of the renormalization scale. Using this normalization one gets after taking the forward matrix element of the expansion in Eq. (13) the representation

$$\Gamma(B \to X_c \bar{\nu}_\ell \ell) = \Gamma^0 |V_{cb}|^2 \left\{ C_0 \left(1 + \frac{\mu_\pi^2}{2m_b^2} \right) + \left(-C_v + \frac{C_G - \tilde{C}_G C_0}{C_{\mathrm{mag}}} \right) \frac{3\Delta m_B^2}{8m_b^2} \right\}. \tag{15}$$

V. DESCRIPTION OF THE CALCULATION AND RESULTS

A. Generalities and techniques

The matching procedure consists in computing matrix elements with partonic states (on-shell quarks and gluons)

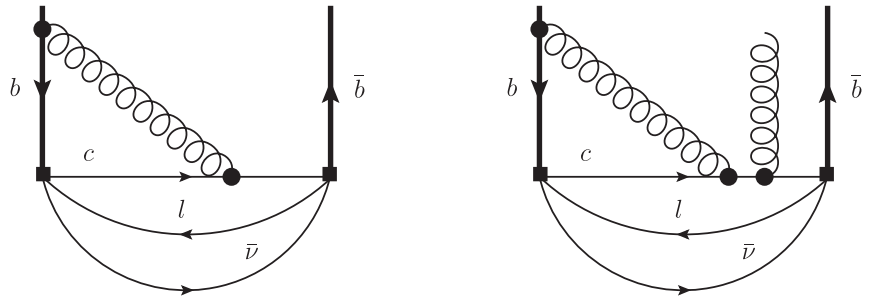

FIG. 1. Perturbation theory diagrams for the matching computation at the NLO level. Left: Partonic type. Right: Power-correction type with the insertion of an external gluon.

on both sides of the relation (11). The coefficient function C_0 of the dimension-three operator $\bar{h}_v h_v$ is the total width of a freely decaying heavy quark, and at the same time the leading contribution to the width of a bottom hadron within HQE techniques. At NLO the calculation of the transition operator $\tilde{T}$ in Eq. (3) requires one to consider three-loop diagrams with external heavy-quark lines on shell. The leading-order result is well known and requires the calculation of the two-loop Feynman integrals of the simplest topology—the sunset-type ones [34]. At the NLO level one needs to compute the on-shell three-loop integrals with massive lines due to the massive c quark. In Fig. 1 we show some typical three-loop diagrams both for the partonic part and power corrections of the decay rate.

The computation has been performed in dimensional regularization, which is used for both ultraviolet and infrared singularities. We used the systems of symbolic manipulations REDUCE [35] and MATHEMATICA [36] with original codes written for the calculation. The package FeynCalc [37] is used for manipulating Dirac matrices and four-vectors in MATHEMATICA. The reduction to master integrals has been done within the integration by parts technique [38]. The original codes have been used for most of the diagrams and then the program LiteRed [39] has been used for checking and further application to complicated diagrams. The master integrals have been computed directly and then checked with the program HypExp [40]. The renormalization is performed on shell by the multiplication of the bare (directly from diagrams) results by the on-shell renormalization constant $Z_2^{\rm OS}$

$$Z_2^{\rm OS} = 1 - C_F \frac{\alpha_s(\mu)}{4\pi}\left(\frac{3}{\epsilon} + 3\ln\left(\frac{\mu^2}{m_b^2}\right) + 4\right). \quad (16)$$

It is convenient to fix the normalization point to the b-quark mass $\mu = m_b$ in the practical computation. The μ dependence can be easily restored from the knowledge of anomalous dimensions.

We use the rest of this section to present the technical details of the calculation and to present our results.

B. The leading power coefficient C_0: partonic width

By using the described methods we reproduce the known result for the heavy-quark width which is given by the contribution of the leading operator $\mathcal{O}_0$. The coefficient C_0 is

$$C_0 = C_0^{\rm LO} + C_F \frac{\alpha_s}{\pi} C_0^{\rm NLO} \quad (17)$$

where the leading-order (LO) contribution reads

$$C_0^{\rm LO} = 1 - 8r - 12r^2\ln(r) + 8r^3 - r^4 \quad (18)$$

and the NLO contribution reads

$$\begin{aligned} C_0^{\rm NLO} = {} & (1-r^2)\left\{\left(\frac{25}{8} - \frac{239}{6}r + \frac{25}{8}r^2\right) + \left(-\frac{17}{6} + \frac{32}{3}r - \frac{17}{6}r^2\right)\ln(1-r)\right\} \\ & + \left(-10 - 45r + \frac{2}{3}r^2 - \frac{17}{6}r^3\right) r\ln(r) + \left(-18 - \frac{r^2}{2}\right) r^2\ln^2(r) \\ & + (2 + 60r^2 + 2r^4)\ln(1-r)\ln(r) + (1 + 16r^2 + r^4)(3{\rm Li}_2(r) - \pi^2/2) \\ & + 16r^{3/2}(1+r)\left(\pi^2 - 4({\rm Li}_2(\sqrt{r}) - {\rm Li}_2(-\sqrt{r})) + 2\ln(r)\ln\frac{1+\sqrt{r}}{1-\sqrt{r}}\right) \end{aligned} \quad (19)$$

with $r = m_c^2/m_b^2$. Here $\mathrm{Li}_2(r)$ is the polylogarithm, $\mathrm{Li}_2(r) = \sum_n r^n/n^2$. The combination

$$r^{1/2}\left(\pi^2 - 4\{\mathrm{Li}_2(\sqrt{r}) - \mathrm{Li}_2(-\sqrt{r})\} + 2\ln(r)\ln\frac{1+\sqrt{r}}{1-\sqrt{r}}\right) \tag{20}$$

is a part of one master integral in the computation and it always appears in this form. It contains a specific contribution $r^{1/2}\pi^2$ with an odd power of m_c (in fact $|m_c|$) while the rest is formally even in m_c. The analytical expression at NLO was first given by Nir [41]. It coincides with that given in Eq. (19).

The behavior near the border of the decay phase space ($r \sim 1$) of the NLO correction

$$C_0^{\mathrm{NLO}}(r \to 1) = \frac{3}{10}(1-r)^5 + O((1-r)^6) \tag{21}$$

is similar to that of the LO which is

$$C_0^{\mathrm{LO}}(r \to 1) = \frac{2}{5}(1-r)^5 + O((1-r)^6). \tag{22}$$

We define the bottom-quark mass to be the pole mass, because it is convenient for computing the relevant matrix elements in QCD with on-shell quark states. The charmed-quark mass can be taken as either the pole mass, or it can be defined in the $\overline{\mathrm{MS}}$ scheme. The relation between the two definitions up to the necessary order is

$$m_c^{\mathrm{pol}} = m_c^{\overline{\mathrm{MS}}}(\mu)\left(1 + C_F\frac{\alpha_s}{4\pi}\left(3\ln\frac{\mu^2}{m_c^2} + 4\right)\right). \tag{23}$$

The numerical value for the charmed-quark mass is best known in the $\overline{\mathrm{MS}}$ scheme [42,43]. It is rather small and cannot be perturbatively cast into the pole mass scheme with any reliable control over uncertainties due to the poor convergence of the perturbative expansion [44]. The numerical value for the bottom-quark mass has been discussed in the literature for a long time and many estimates are available. In addition, there is an extensive discussion on what particular scheme of defining the quark mass parameter is the most suitable one for this particular observable [45,46].

In Fig. 2 we give the plot of the coefficient $C_0^{\mathrm{LO}}(r)$ and also the normalized next-to-leading coefficient $\hat{C}_0^{\mathrm{NLO}}(r)$ in the pole mass scheme for m_c.

In Fig. 3 we give the plot of the mass dependence of the coefficient $C_0^{\mathrm{NLO}}(r)$ in different mass schemes for m_c. In phenomenological applications the $\overline{\mathrm{MS}}$-scheme definition of the charm-quark mass is usually used.

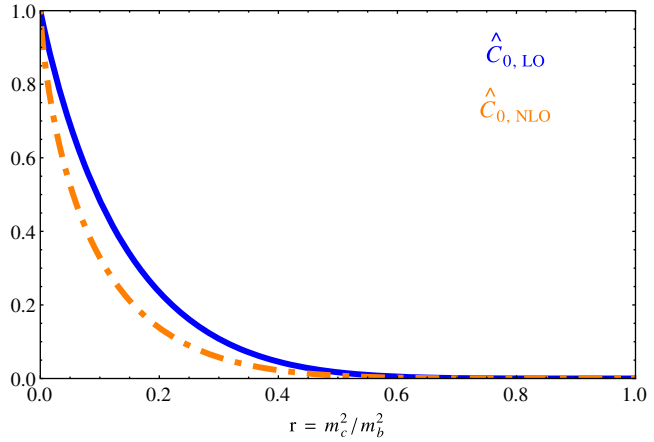

FIG. 2 (color online). The mass dependence of the coefficient $C_0(r)$ in the pole mass scheme for m_c at LO (solid line) and NLO (dash-dotted line) normalized to $C_0^{\mathrm{NLO}}(0)$: $\hat{C}_0^{\mathrm{NLO}}(r) = C_0^{\mathrm{NLO}}(r)/C_0^{\mathrm{NLO}}(0)$, $\hat{C}_0^{\mathrm{LO}}(r) = C_0^{\mathrm{LO}}(r)$.

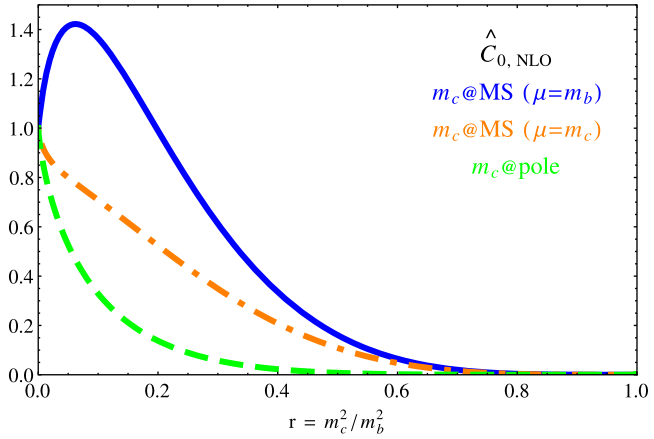

FIG. 3 (color online). Mass dependence of the coefficient $C_0^{\mathrm{NLO}}(r)$ in the pole and $\overline{\mathrm{MS}}$ schemes with $\mu = m_b$ and $\mu = m_c$.

In the small-mass limit for the charmed quark one finds

$$C_0^{\mathrm{NLO}}(r)|_{r\to 0} = \left(\frac{25}{8} - \frac{\pi^2}{2}\right) - 2r(6\ln(r) + 17) + 16\pi^2 r^{3/2} + O(r^2\ln^2 r). \tag{24}$$

We have computed the results for the coefficient C_0 in the massless limit, $C_0(0)$, independently which serves partly as a check of our full mass calculation.

The relative magnitude of the NLO contribution at a typical value of the mass ratio $r = 0.07$ is

$$C_0(0.07) = 0.60 - 0.78C_F\frac{\alpha_s}{\pi} = 0.6\left(1 - C_F\frac{\alpha_s}{\pi}1.31\right) \tag{25}$$

while in the massless limit it is

$$C_0(0) = 1 - C_F \frac{\alpha_s}{\pi} 1.8. \tag{26}$$

The numerical value for the bottom-quark mass m_b is important for phenomenological applications and has been discussed in the literature (see, e.g. Ref. [45]). The dependence on the charm-quark mass is essential but it still mainly follows the pattern of that at leading order. This similarity supports the idea of Ref. [21] that the computation in the massless limit can be useful for physical applications as the normalization and the extrapolation with the leading-order massive result can be a reasonable approximation for the mass dependence at NLO. We will see how it works or does not work for other coefficients later.

C. The *vD*-operator coefficient C_v

In this subsection we present the result for the coefficient C_v which is an auxiliary quantity in our approach since the operator is reexpressed through the other contributions at the level of matrix elements. The coefficient C_v is singled out by taking the matrix element between b quarks on shell and one gluon with vanishing momentum and longitudinal polarization, i.e. the gluon field is chosen in the form $A_\mu = v_\mu (vA)$. Here A_μ is a matrix in color space $A_\mu = A_\mu^a t^a$. The result for the coefficient C_v

$$C_v = C_v^{\rm LO} + C_F \frac{\alpha_s}{\pi} C_v^{\rm NLO} \tag{27}$$

reads

$$C_v^{\rm LO} = 5 - 24r - 12r^2 \ln(r) + 24r^2 - 8r^3 + 3r^4.$$

In Fig. 4 we plot the charmed-quark mass dependence of C_v.

For the NLO part $C_v^{\rm NLO}$ we give explicitly only the expression for the small-r expansion. The structure of the whole contribution is very similar to that of $C_0^{\rm NLO}$. The expression is rather long and given in Appendix B. Its small-mass expansion reads

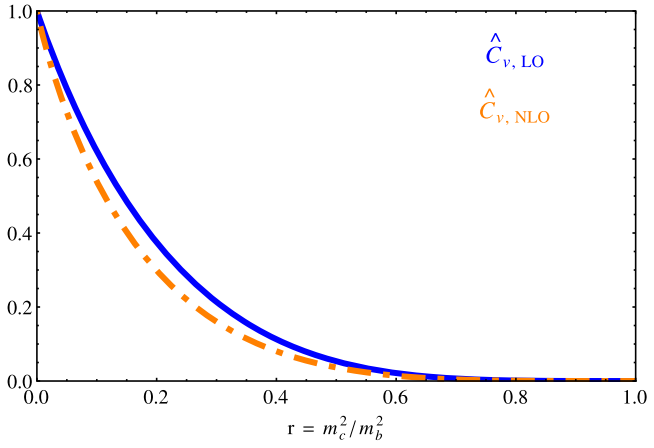

FIG. 4 (color online). Mass dependence of the coefficient $C_v(r)$.

$$C_v^{\rm NLO} = \left(-\frac{25}{24} - \frac{\pi^2}{2}\right) + 48r - 8\pi^2 r^{3/2} + O(r^2 \ln^2 r). \tag{28}$$

The leading term of the expression coincides with the independent computation in the massless limit done in Ref. [21]

$$C_v|_{r=0} = 5 + C_F \frac{\alpha_s}{\pi} \left\{-\frac{25}{24} - \frac{\pi^2}{2}\right\}. \tag{29}$$

For the mass dependence of the coefficient C_v, for the typical value of $r = 0.07$, one finds

$$C_v(0.07) = 3.6 - 3.8 C_F \frac{\alpha_s}{\pi} = 3.6\left(1 - C_F \frac{\alpha_s}{\pi} 1.1\right) \tag{30}$$

while in the massless limit one has

$$C_v(0) = 5\left(1 - C_F \frac{\alpha_s}{\pi} 1.2\right). \tag{31}$$

One sees again a rather reasonable accuracy for the extrapolation to $m_c \neq 0$ at NLO.

The coefficient C_v has no C_A color structure; it contains only the C_F color group invariant. This property matches the possibility to compute this coefficient using a small-momentum expansion near the quark mass shell, $p = mv + k$. Still, an explicit cancellation of the contribution proportional to the color structure C_A and a cancellation of poles with the same renormalization constant $Z_2^{\rm OS}$ shown in Eq. (16) is a powerful check of the final result.

The large-m_c behavior at the border of phase space is

$$C_v^{\rm NLO}(r \to 1) = -3(1-r)^4 + O((1-r)^5) \tag{32}$$

and

$$C_v^{\rm LO}(r \to 1) = 4(1-r)^4 + O((1-r)^5). \tag{33}$$

D. The coefficient $C_G - C_0 \tilde{C}_G \equiv C_G^r$: chromomagnetic operator

For the chromomagnetic-operator coefficient we directly compute the difference between contributions to the width correlator in Eq. (11) and the local $\bar{b}\not{x}b$ operator in Eq. (12) multiplied by the leading power coefficient $C_0(r)$, $C_G^r = C_G - C_0 \tilde{C}_G$. We write this coefficient as a sum of a leading-order term and a radiative correction in the form

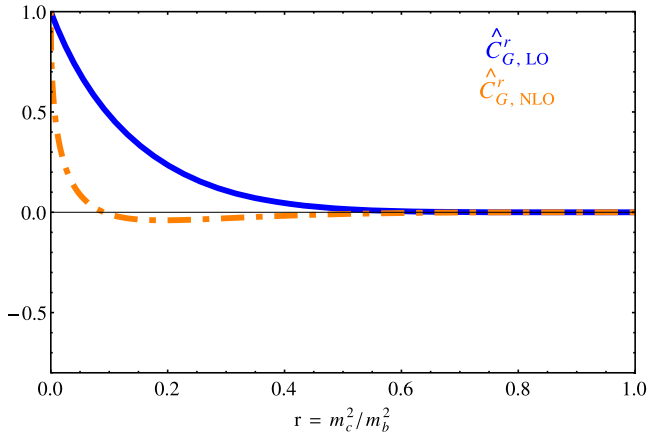

FIG. 5 (color online). Mass dependence of the coefficient $C^r_G = C_G - C_0\tilde{C}_G$ with $\mu = m_b$.

$$C^r_G(r) = C^{r,\mathrm{LO}}_G(r) + \frac{\alpha_s}{\pi}\left\{C_A C^{r,\mathrm{NLO},A}_G(r) + C_F C^{r,\mathrm{NLO},F}_G(r)\right\} \tag{34}$$

where the NLO coefficient is separated into two color structures with C_A and C_F color group invariants. In Fig. 5 we present the plot of the mass dependence for the coefficient of the chromomagnetic operator for QCD with $C_A = 3$ and $C_F = 4/3$. One sees that the mass dependence of C^r_G at NLO is much sharper than in previous cases. This is unexpected and makes the conjecture used in Ref. [21] about a uniform phas- space suppression for the coefficients less accurate. The explicit leading-order expression reads

$$C^{r,\mathrm{LO}}_G = 2 - 16r - 24r^2\ln(r) + 16r^3 - 2r^4 = 2C^{\mathrm{LO}}_0. \tag{35}$$

The NLO coefficients with full mass dependence are too long to be displayed here, whereas the expanded results are

$$C^{r,\mathrm{NLO},A}_G = -\frac{8\pi^2\sqrt{r}}{3} + r\left(\ln^2(r) - 25\ln(r) + \frac{2\pi^2}{3} - 25\right) - \frac{\pi^2}{9} + \frac{49}{18},$$
$$C^{r,\mathrm{NLO},F}_G = \frac{32\pi^2\sqrt{r}}{3} + r(-4\ln^2(r) + 68\ln(r) - 4\pi^2 + 21) - \frac{7\pi^2}{9} - \frac{47}{36}. \tag{36}$$

At the border of phase space we obtain

$$C^{r,\mathrm{NLO}}_G(r\to 1) = C_F(1-r)^4 + \frac{1}{5}[2C_F - 3C_A](1-r)^5 + O((1-r)^6) \tag{37}$$

and

$$C^{r,\mathrm{LO}}_G(r\to 1) = \frac{4}{5}(1-r)^5 + O((1-r)^6). \tag{38}$$

In the massless limit the C^r_G coefficient is given by

$$C^r_G(0) = 2 + \frac{\alpha_s}{\pi}\left\{C_A\left(\frac{49}{18} - \frac{\pi^2}{9}\right) + C_F\left(-\frac{47}{36} - \frac{7\pi^2}{9}\right)\right\}. \tag{39}$$

This result has been independently determined by direct computation using the technology developed for the massless case.

E. COEFFICIENT $C_{\bar{\mu}^2_G} = -C_v + C^r_G/C_{\mathrm{mag}}$: THE MATRIX ELEMENT OF $C_{\mathrm{mag}}\mathcal{O}_G$

This coefficient is the final result after the use of the equations of motion. We prefer to place the coefficient in front of the renormalization-group-invariant combination

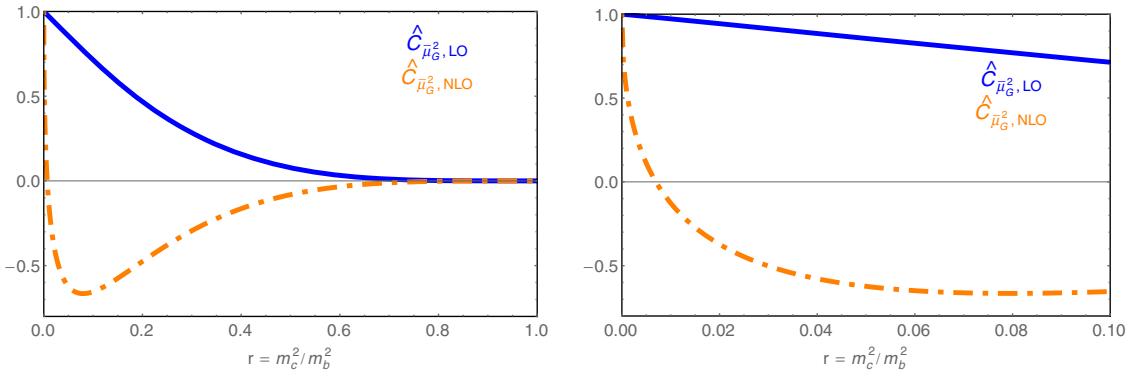

FIG. 6 (color online). The mass dependence of the coefficient $C_{\bar{\mu}^2_G}(r)$ at LO and NLO in the pole mass scheme. QCD color factors: $C_A = 3$, $C_F = 4/3$. Left panel: The whole phase space. Right panel: Zoomed image of the small-mass region $0 < r < 0.1$.

that enters the HQET Lagrangian. This combination also determines the mass splitting in the ground-state multiplets due to spin orientation.

Thus, the final coefficient of the matrix element of the chromomagnetic operator with account of the equation of motion after taking the hadronic matrix elements reads

$$C_{\bar{\mu}_G^2}(r) = -C_v(r) + \frac{C_G^r(r)}{C_{\rm mag}(\mu)}. \tag{40}$$

This is a coefficient in front of the matrix element of the renormalization-invariant combination $C_{\rm mag}(\mu)\mathcal{O}_G(\mu)$.

In Fig. 6 we plot the mass dependence of this final coefficient.

Writing again the decomposition of the whole coefficient at NLO

$$C_{\bar{\mu}_G^2}(r) = C_{\bar{\mu}_G^2}^{\rm LO} + \frac{\alpha_s}{\pi}\{C_A C_{\bar{\mu}_G^2}(r)^{{\rm NLO},A} + C_F C_{\bar{\mu}_G^2}(r)^{{\rm NLO},F}\} \tag{41}$$

we obtain at the leading order the well-known result

$$C_{\bar{\mu}_G^2}^{\rm LO} = -3 + 8r - 24r^2 - 12r^2\ln(r) + 24r^3 - 5r^4. \tag{42}$$

The complete expressions are given in Appendix C. Here we present the new result at NLO as a small-r expansion only

$$\begin{aligned} C_{\bar{\mu}_G^2}^{{\rm NLO},A} &= \frac{2\pi^2 r}{3} - 17r - \frac{8\pi^2\sqrt{r}}{3} + r\log^2(r) \\ &\quad - 25r\log(r) - \frac{\pi^2}{9} + \frac{31}{18}, \\ C_{\bar{\mu}_G^2}^{{\rm NLO},F} &= -4\pi^2 r - 19r + \frac{32\pi^2\sqrt{r}}{3} - 4r\log^2(r) \\ &\quad + 68r\log(r) - \frac{5\pi^2}{18} - \frac{91}{72}. \end{aligned} \tag{43}$$

After inserting the QCD color factors $C_A = 3$, $C_F = 4/3$ one gets

$$\begin{aligned} C_{\bar{\mu}_G^2}^{\rm NLO} &= \left(\frac{94}{27} - \frac{19\pi^2}{27}\right) + \frac{56\pi^2\sqrt{r}}{9} \\ &\quad + \frac{1}{3}r(-7\ln^2(r) + 47\ln(r) - 10\pi^2 - 229) + \frac{280}{27}\pi^2 r^{3/2} \\ &\quad + \frac{1}{81}r^2(-1251\ln^2(r) - 1917\ln(r) - 216\pi^2 - 5750) \\ &\quad + O(r^{5/2}). \end{aligned} \tag{44}$$

The very large contribution of the $\sqrt{r}$ term leads to a very fast change of the coefficient $C_{\bar{\mu}_G^2}^{\rm NLO}$ from its massless limit value with an increase of the charm-quark mass. Numerically one finds

$$\begin{aligned} C_{\bar{\mu}_G^2}^{\rm NLO} &= -3.46 + 61.41\sqrt{r} + r(-2.3\ln^2(r) \\ &\quad + 15.7\ln(r) - 109.2) + O(r^{3/2}). \end{aligned} \tag{45}$$

In the massless limit the new result is

$$C_{\bar{\mu}_G^2} = -3 + \frac{\alpha_s}{\pi}\left\{C_A\left(\frac{31}{18} - \frac{\pi^2}{9}\right) - C_F\left(\frac{91}{72} + \frac{5\pi^2}{18}\right)\right\}.$$

Note that the C_F part of this coefficient differs from the result given in Ref. [21]. The difference is given by $2C_0^{\rm NLO}$ and it emerged because in Ref. [21] only the leading order of the C_0 coefficient was used for subtracting the contribution of the local $\bar{b}\not{v}b$ operator.

The μ dependence of the prefactor of $\mathcal{O}_G$ in Eq. (13) matches the leading-order anomalous dimension of the chromomagnetic operator [30], such that $C_{\bar{\mu}_G^2}$ is μ independent.

The end-of-spectrum behavior reads

$$\begin{aligned} C_{\bar{\mu}_G^2}^{\rm NLO}(r \to 1) &= 4C_F(1-r)^4 \\ &\quad + \left[\frac{3}{10}C_F - C_A\right](1-r)^5 + O((1-r)^6) \end{aligned} \tag{46}$$

for NLO and

$$C_{\bar{\mu}_G^2}^{\rm LO}(r \to 1) = -4(1-r)^4 + O((1-r)^6) \tag{47}$$

for the LO contribution.

The mass parameter of the heavy quark m_b is chosen to be the pole mass which is a proper formal parameter for perturbative computations in HQET (see the discussion in Ref. [26]). After having obtained the results of the perturbation theory computation for the coefficients of HQE, one is free to change this parameter to any other choice [46].

VI. DISCUSSION OF THE RESULTS

A. The total width

The radiative corrections are of reasonable magnitude and are well under control for the numerical values of the coupling constant for $\mu \sim 2$–4 GeV (for the numerical value see, e.g. Ref. [47]). This provides a clean application of the results to phenomenology. However, the final quark-mass dependence is remarkable. It is very steep for small m_c and therefore the decays into light quarks u for bottom mesons and d for charmed mesons should be treated with care.

The coefficients of HQE have been also calculated in Ref. [20] where the analytical computation has been performed for the hadronic tensor and the final integration over the phase space has been done numerically.

Such a setup has advantages for direct comparison with experimental data since the experimental cuts in the phase space can be readily introduced.

We can make a literal comparison with the results of Ref. [20] for the total width. Our result in the format of Ref. [20] is

$$\Gamma = \Gamma_0^m\left(\left(1-1.7776\frac{\alpha_s}{\pi}\right)\left(1-\frac{\mu_\pi^2}{2m_b^2}\right) - (1.9449+2.4235\frac{\alpha_s}{\pi})\frac{\mu_G^2}{m_b^2}\right) \tag{48}$$

for $r = 0.0625$ which literally coincides with the results of Ref. [20].

For phenomenological applications and comparison with experiment within our approach one can compute moments of the differential distribution (see, e.g. Ref. [48]). It is straightforward to compute almost any moment in the invariant lepton pair mass, lepton pair energy or invariant mass of the hadronic system. We present a few such moments below.

B. Moments of the differential distribution

Note that our computation is organized such that it allows for the computation of certain moments of the differential distribution. We can build up moments over the leptonic pair invariant mass squared q^2, $(q = p_\ell + p_\nu)$ and the partonic invariant mass squared $(p-q)^2$, where p is the momentum of the bottom quark and $p = m_b v$. This is possible because we have the leptonic part and the partonic parts separately in an intermediate representation of computed diagrams—one can compute the moments in q^2 and/or in $(p-q)^2$. The total lepton energy moments (the moments in the variable pq) are just the linear combinations of those two sets. We present the analytical results for a few moments in the small-r expansion for brevity. The analytical expression for the total width is given for further comparison with the moments. It reads

$$\begin{aligned}\Gamma/\Gamma_0 = {} & 1-8r+C_F\frac{\alpha_s}{4\pi}\left(\frac{25}{2}-2\pi^2-8r(6\ln(r)+17)\right)\\ & +\frac{\bar\mu_G^2}{2m_b^2}\left\{-3+8r+\frac{\alpha_s}{4\pi}\times\left(C_A\left(\frac{2\pi^2 r}{3}-17r-\frac{8\pi^2\sqrt{r}}{3}+r\ln^2(r)-25r\ln(r)-\frac{\pi^2}{9}+\frac{31}{18}\right)\right.\right.\\ & \left.\left.+C_F\left(-4\pi^2 r-19r+\frac{32\pi^2\sqrt{r}}{3}-4r\ln^2(r)+68r\ln(r)-\frac{5\pi^2}{18}-\frac{91}{72}\right)\right)\right\}\end{aligned} \tag{49}$$

where $\bar\mu_G^2 = C_{\rm mag}(\mu)\mu_G^2(\mu)$.

The normalized q^2 moments of the total width with the $C_{\bar\mu_G^2}$ coefficient are given below. For convenience they are normalized to unity at leading order of the power, small mass, and perturbative expansions. The normalization can be obtained independently. Indeed, the $x = q^2/m_b^2$ distribution in the massless limit at LO is given by

$$\frac{1}{\Gamma_0}\frac{d\Gamma}{dx} = 2(1-x)(1+2x). \tag{50}$$

The normalization factors for the moments $n = 1$–3 are then $N(M_n^q) = \{3/10, 2/15, 1/14\}$. For example,

$$N(M_1^q) = \int_0^1 2(1-x)(1+2x)xdx = 3/10. \tag{51}$$

The first moment $(q^2/m_b^2)^1$ is

$$\begin{aligned}M_1^q = {} & 1-15r+C_F\frac{\alpha_s}{4\pi}\left(13-2\pi^2-r\left(90\ln(r)+\frac{10\pi^2}{9}+355\right)\right)\\ & +\frac{\bar\mu_G^2}{2m_b^2}\left(-\frac{25}{3}+\frac{\alpha_s}{\pi}\left(C_A\left(-\frac{80\pi^2\sqrt{r}}{9}-\frac{25\pi^2}{27}+\frac{260}{27}\right)+C_F\left(\frac{320\pi^2\sqrt{r}}{9}+\frac{65\pi^2}{54}-\frac{763}{36}\right)\right)\right).\end{aligned}$$

The second moment $(q^2/m_b^2)^2$ is

$$\begin{aligned}M_2^q = {} & 1-24r+C_F\frac{\alpha_s}{4\pi}\left(\frac{604}{45}-2\pi^2+r\left(-144\ln(r)-2\pi^2-\frac{6813}{10}\right)\right)\\ & +\frac{\bar\mu_G^2}{2m_b^2}\left(-15+\frac{\alpha_s}{\pi}\left(C_A\left(-20\pi^2\sqrt{r}-\frac{17\pi^2}{12}+\frac{541}{40}\right)+C_F\left(80\pi^2\sqrt{r}+\frac{7\pi^2}{3}-41\right)\right)\right).\end{aligned} \tag{52}$$

The third moment $(q^2/m_b^2)^3$ is

$$M_3^q = 1 - 35r + C_F\frac{\alpha_s}{4\pi}\left(\frac{1243}{90} - 2\pi^2 + r\left(-210\log(r) - \frac{14\pi^2}{5} - \frac{20195}{18}\right)\right) + \frac{\bar{\mu}_G^2}{2m_b^2}\left(-23 + \frac{\alpha_s}{\pi}\left(C_A\left(-\frac{112\pi^2\sqrt{r}}{3} - \frac{35\pi^2}{18} + \frac{27217}{1620}\right) + C_F\left(\frac{448\pi^2\sqrt{r}}{3} + \frac{67\pi^2}{18} - \frac{1088429}{16200}\right)\right)\right).$$

The q^2 moments are very stable and hardly change with n besides the total normalization. Usually one argues that radiative corrections should increase or decrease depending on the momentum flow through the diagram—we see no simple explanation for the change of radiative corrections.

The moments in the partonic variable $(p-q)^2 - m_c^2$ are defined through the relation

$$M_n^H = \int \frac{((p-q)^2 - m_c^2)^n}{m_b^{2n}}\frac{d\Gamma}{\Gamma_0} \tag{53}$$

and have been considered in Ref. [48]. They are given below for $n = 1$–3 analytically within the small-r expansion.

The first moment $((p-q)^2 - m_c^2)^1$ is

$$M_1^H = C_F\frac{\alpha_s}{\pi}\left(\frac{71r}{24} + \frac{3}{2}r\log(r) + \frac{91}{600}\right) + \frac{\bar{\mu}_G^2}{2m_b^2}\left(\frac{\alpha_s}{\pi}\left(C_A\left(-\frac{611r}{108} - \frac{22}{9}r\log(r) - \frac{29}{180}\right) + C_F\left(-\frac{73\pi^2 r}{36} + \frac{457r}{108} - \frac{67}{36}r\log(r) - \frac{\pi^2}{4} + \frac{77}{45}\right)\right) - \frac{3r}{2} + \frac{1}{2}\right). \tag{54}$$

The second moment $((p-q)^2 - m_c^2)^2$ is

$$M_2^H = C_F\frac{\alpha_s}{\pi}\left(\frac{5}{432} - \frac{137r}{600}\right) + \frac{\bar{\mu}_G^2}{2m_b^2}\frac{\alpha_s}{\pi}\left(C_A\left(r\left(\frac{\ln(r)}{18} + \frac{163}{1080}\right) + \frac{1}{72}\right) + C_F\left(r\left(\frac{25\ln(r)}{18} + \frac{3703}{1080}\right) + \frac{347}{3600}\right)\right). \tag{55}$$

The third moment $((p-q)^2 - m_c^2)^3$ is

$$M_3^H = C_F\frac{\alpha_s}{\pi}\left(\frac{377}{176400} - \frac{119r}{3600}\right) + \frac{\bar{\mu}_G^2}{2m_b^2}\frac{\alpha_s}{\pi}\left(C_A\frac{43}{16200} + C_F\frac{11537}{1587600}\right).$$

This set is such that moments vanish at leading order. Therefore one cannot discuss the relative magnitude of radiative corrections. Our results for $n = 1$–2 coincide with those of Ref. [48].

We also compute the relevant moments numerically with full mass dependence for a typical value of the mass ratio. For the q^2 moments up to third order we obtain with $r = 0.0625$

$$\begin{aligned} M_0^q &= \left(1 - 1.7776\frac{\alpha_s}{\pi}\right) - 3.8898\left(1 - 0.9206\frac{\alpha_s}{\pi}\right)\frac{\bar{\mu}_G^2}{2m_b^2}, \\ M_1^q &= \left(1 - 1.6500\frac{\alpha_s}{\pi}\right) - 8.9901\left(1 - 0.6834\frac{\alpha_s}{\pi}\right)\frac{\bar{\mu}_G^2}{2m_b^2}, \\ M_2^q &= \left(1 - 1.5575\frac{\alpha_s}{\pi}\right) - 14.394\left(1 - 0.5578\frac{\alpha_s}{\pi}\right)\frac{\bar{\mu}_G^2}{2m_b^2}, \\ M_3^q &= \left(1 - 1.4847\frac{\alpha_s}{\pi}\right) - 19.997\left(1 - 0.4666\frac{\alpha_s}{\pi}\right)\frac{\bar{\mu}_G^2}{2m_b^2}. \end{aligned} \tag{56}$$

Numerically for partonic moments in $H = (p-q)^2 - m_c^2$ with $r = 0.0625$ one obtains

$$M_1^H = 0.0569\frac{\alpha_s}{\pi} + 0.397\left(1 - 2.304\frac{\alpha_s}{\pi}\right)\frac{\bar{\mu}_G^2}{2m_b^2},$$
$$M_2^H = 0.00575\frac{\alpha_s}{\pi} + 0.0554\frac{\alpha_s}{\pi}\frac{\bar{\mu}_G^2}{2m_b^2},$$
$$M_3^H = 0.00114\frac{\alpha_s}{\pi} + 0.00694\frac{\alpha_s}{\pi}\frac{\bar{\mu}_G^2}{2m_b^2}, \quad (57)$$

with $\bar{\mu}_G^2 = C_{\rm mag}(\mu)\mu_G^2(\mu)$.

It is also possible to compute the moments of the lepton energy spectrum that are of interest from the experimental point of view. However, here a few more technical problems arise. On the one hand the whole set up of the analytical calculation has to be modified, since the leptonic tensor has to be taken as a differential distribution rather than fully integrated over the lepton phase space. On the other hand there is the question of how to deal with γ_5 in dimensional regularization. For the cases we discussed here we always have a situation when there is an even (in fact two) number of γ_5 matrices within the trace over Dirac matrices both in the leptonic and hadronic parts, so we simply and consistently use anticommuting γ_5. However, in the calculation of the moments of the charged-lepton energy one also has to consider an odd number of γ_5 matrices in the traces, which causes an additional complication of the calculation. Nevertheless, with the technology developed here, these problems can be tackled and we plan to present a calculation of lepton-energy moments in a separate publication.

C. Phenomenological outlook

This paper has been devoted to the description of the technical aspects of the calculation of the perturbative QCD corrections for subleading powers in the $1/m$ expansion. Aside from a more theoretical consideration, such as the discussion of the mass dependence of the various terms of the HQE, such a calculation has a variety of phenomenological applications, of which the most prominent one is its application to inclusive semileptonic $b \to c$ transitions.

These decays are currently believed to be the most precise method to determine the CKM matrix element V_{cb}. In this method, V_{cb} is extracted form the heavy quark expansion for the total rate, while the HQE parameters μ_π, ρ_D etc. are extracted from the moments of the differential rates. Based on this methodology, the theoretical uncertainty in V_{cb} has been reduced to a level below 1%, while the total uncertainty (including the experimental uncertainty as well as the uncertainty in the extraction of the HQE parameters) is at the level of 2%. As it has been shown in Ref. [49] the impact of the $\alpha_s\mu_G^2$ contribution is in fact of the expected size, shifting the central value of V_{cb} by about -0.5%.

From the experimental side, the lepton energies cannot be measured to arbitrarily low values. Thus either an extrapolation is necessary or one has to include a cut in the theoretical predictions. Since an extrapolation involves a model dependence, it is more favorable to include a lepton-energy cut in the theoretical prediction. However, unlike in the numerical study of Refs. [20,50], such a cut cannot be implemented in an analytical calculation, at least not exactly. Thus in order to make phenomenological use of the analytical calculation one needs to take into account the effects of such a cut, which needs further study. We plan to return to this in a separate publication.

ACKNOWLEDGMENTS

We acknowledge discussions with A. G. Grozin, B. O. Lange, J. Heinonen, and T. Huber. We thank P. Gambino for communication on their ongoing work on radiative corrections to inclusive weak decays. This work is supported by the Deutsche Forschungsgemeinschaft (DFG) within research unit FOR 1873 "Quark Flavors Physics and Effective Theories."

APPENDIX A: MASTER INTEGRALS

In this section we present the results for the master integrals entering our calculation in the dimensional regularization with $D = 4 - 2\varepsilon$. The general integral

$$S(a,b;m^2,p^2) = \frac{1}{i\pi^{D/2}}\int\frac{d^Dk}{(m^2-k^2)^a(-(p-k)^2)^b} \quad (A1)$$

develops a cut at $p^2 = s > m^2$ with a discontinuity $\rho(a,b;m^2,s)$ that is

$$\rho(a,b;m^2,s) = \frac{1}{2\pi i}(S(a,b;m^2,s+i0) - S(a,b;m^2,s-i0)). \quad (A2)$$

It is a spectrum of a general sunset diagram [34]

$$\rho(a,b;m^2,s) = \frac{\Gamma(D/2-b)}{\Gamma(a)\Gamma(b)\Gamma(D-a-2b+1)} z^{D-a-2b}s^{D/2-a-b}{}_2F_1(D/2-b,1-b;D-a-2b+1;z) \quad (A3)$$

with $z = 1 - m^2/s$. Here ${}_2F_1(a,b;c;z)$ is a hypergeometric function. In our case $m = m_c$ and $s = m_b^2$.

1. Master integrals at LO: two loop

At LO there are two master integrals. In both cases it is a two-loop sunset with one heavy (m_c) line. The internal

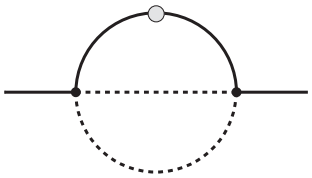

FIG. 7. Two-loop master integral. A dotted line indicates one additional power of the propagator.

massive line can be a normal one or doubled which is denoted by a dot; see Fig. 7.

The closed form for a master integral with a normal line is

$$M_{00} = S(1,1;0,-1)\rho(1,2-D/2;m_c^2,m_b^2) \quad \text{(A4)}$$

where $S(1,1;0,-1)$ is a scalar massless loop that is expressible through Γ functions

$$S(a,b;0,-1) = \frac{\Gamma(a+b-D/2)\Gamma(D/2-a)\Gamma(D/2-b)}{\Gamma(a)\Gamma(b)\Gamma(D-a-b)}. \quad \text{(A5)}$$

We usually set $m_b = 1$ in the computation. The ε expansion of this integral can be obtained with the program HypExp or independently. At the leading order of the ε expansion one has

$$M_{00} = \frac{1}{2} + m^2\ln(m^2) - \frac{m^4}{2} + O(\varepsilon) \quad \text{(A6)}$$

with $m = m_c$ and $m_b = 1$.

The second master integral (dotted) belongs to the same class of sunsets and can be obtained as a derivative in m_c

$$M_{01} = -\frac{d}{dm_c^2}M_{00}. \quad \text{(A7)}$$

The closed form for this dotted leading-order master integral is

$$M_{01} = S(1,1;0,-1)\rho(2,2-D/2;m_c^2,m_b^2). \quad \text{(A8)}$$

2. Master integrals at NLO: three loop

At NLO there are master integrals that are factorizable, of sunset type, and nontrivial.

a. Factorizable integrals

The factorized master integrals contain a closed massive loop that can be a loop of either a charmed quark or a bottom quark; Fig. 8.

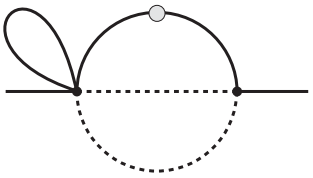

FIG. 8. Factorizable three-loop master integrals.

These master integrals are

$$M_{11} = T_0(m_c)M_{00} \quad \text{(A9)}$$

with $T_0(m)$ being a massive tadpole

$$T_0(m) = m^{D-2}\Gamma(1-D/2) \quad \text{(A10)}$$

and the other one is

$$M_{12} = T_0(m_c)M_{01}. \quad \text{(A11)}$$

The master integrals with a b-quark tadpole are

$$M_{41} = T_0(m_b)M_{00} \quad \text{(A12)}$$

and the other one is

$$M_{42} = T(m_b)M_{01}. \quad \text{(A13)}$$

In the actual computation the bottom-quark mass is set to unity.

b. Sunset-type integrals

The nonfactorizable but still simple master integrals M_{21}, M_{22} are of the sunset type; Fig. 9.

The normal one is given by the basic integral

$$M_{21} = S(1,1;0,-1)S(1,2-D/2;0,-1)\rho(1,3-D,m_c^2,m_b^2). \quad \text{(A14)}$$

The dotted one is its derivative in the loop (charmed-quark) mass

$$M_{22n} = -\frac{d}{dm_c^2}M_{21} \quad \text{(A15)}$$

which is again a three-loop sunset

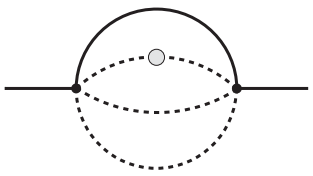

FIG. 9. Sunset-type three-loop master integrals.

$$M_{21} = S(1,1;0,-1)S(1,2-D/2;0,-1)\rho(2,3-D,m_c^2,m_b^2). \quad \text{(A16)}$$

c. Nontrivial master integrals

There are two nontrivial master integrals that can be chosen in a variety of ways. We define the first nontrivial master integral N_p as a sum of the left (dotted at the bottom line) and right (dotted on the charm line) diagrams in Fig. 10. This can be expressed in words as $N_p = dot.m_b + dot.m_c$.

We managed to compute the ε expansion of N_p up to a necessary order. It reads

$$N_p = N_p^{\mathrm{LO}} + \varepsilon N_p^{\mathrm{NLO}} \quad \text{(A17)}$$

with

$$N_p^{\mathrm{LO}} = -2(1-r) - (1+r)\log(r) \quad \text{(A18)}$$

and

$$N_p^{\mathrm{NLO}} = 4\sqrt{r}\left(4(\mathrm{Li}_2(-\sqrt{r}) - \mathrm{Li}_2(\sqrt{r})) + \pi^2 + 2\ln(r)\ln\frac{\sqrt{r}+1}{1-\sqrt{r}}\right) + \left(\frac{1}{2} - \frac{r}{2}\right)\ln^2(r) - 3(r+1)\ln(r) + 4(r+1)\ln(1-r)\ln(r) + 8(1-r)\ln(1-r) + 14(r-1). \quad \text{(A19)}$$

These are master integrals entering the partonic contribution for the total width and the C_v coefficient.

At NLO one more master integral appears to be necessary for the C_G coefficient. It is represented by the difference of the left and right diagrams in Fig. 10. This can be expressed in words as $N_m = dot.m_b - dot.m_c$. We need only the leading term of its ε expansion which reads

$$N_m = (1-r)\left(-4\mathrm{Li}_2(r) + \frac{2\pi^2}{3} - 4\ln(1-r)\ln(r) + 2\ln(r)\right) - 2r\ln^2(r). \quad \text{(A20)}$$

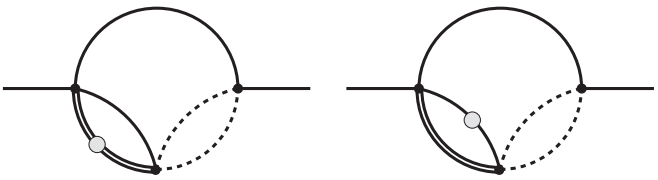

FIG. 10. Nontrivial three-loop master integrals.

3. Master integrals in the massless case

We have calculated all quantities in the massless limit independently. The reduction procedure and master integrals have been obtained independently as well. In the massless case master integrals can be found in a concise form. These master integrals are represented by the Feynman diagrams given in Fig. 11.

At leading order there is one master integral

$$M_{00}^0 = S(1,1;0,-1)S(1,2-D/2;0,-1)\frac{\sin(2\pi\varepsilon)}{\pi}. \quad \text{(A21)}$$

At NLO in the massless case there are three master integrals:

(a) a factorizable integral

$$M_{11}^0 = T_0(m_b)M_{00}^0; \quad \text{(A22)}$$

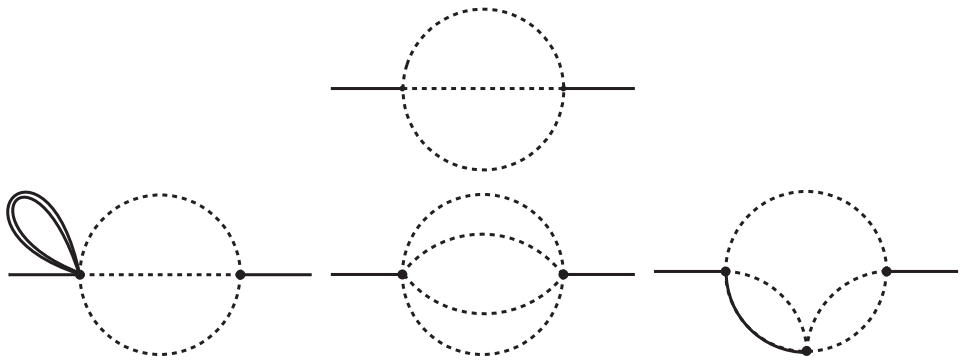

(a) (b) (c)

FIG. 11. Massless two- and three-loop master integrals.

(b) a sunset integral

$$M_{21}^0 = S(1,1;0,-1)S(1,2-D/2;0,-1)S(1,3-D;0,-1)\frac{\sin(3\pi\varepsilon)}{\pi}; \tag{A23}$$

(c) a complicated integral

$$N^0 = -S(1,1;0,-1)\frac{\Gamma(1-\varepsilon)^2}{\Gamma(2-\varepsilon)\Gamma(3-3\varepsilon)}\,{}_3F_2(\{\varepsilon,1-\varepsilon,1\};\{3-3\varepsilon,2-\varepsilon\},1), \tag{A24}$$

where ${}_3F_2(\{\varepsilon,1-\varepsilon,1\};\{3-3\varepsilon,2-\varepsilon\},1)$ is a ${}_pF_q$-type hypergeometric function.

APPENDIX B: C_v COEFFICIENT AT NLO WITH FULL MASS DEPENDENCE

The expression for the coefficient C_v is

$$\begin{aligned}
C_v^{\rm NLO} = &\left(3{\rm Li}_2(r) - \frac{1}{2}\pi^2\right)(1-16r^2-3r^4) - \frac{1}{24}(1-r)(25-1011r-1487r^2+189r^3)\\
&+\frac{1}{6}r(12+450r+4r^2+45r^3)\ln(r) - \frac{1}{6}(1-r)(11+11r+83r^2-45r^3)\ln(1-r)\\
&+\frac{3}{2}r^2(4+r^2)\ln^2(r) + 2(1-30r^2-3r^4)\ln(1-r)\ln(r)\\
&+8r^{3/2}(1+3r)\left(4{\rm Li}_2^- - \pi^2 - 2\ln\left(\frac{1+\sqrt{r}}{1-\sqrt{r}}\right)\ln(r)\right)
\end{aligned} \tag{B1}$$

where ${\rm Li}_2^- = {\rm Li}_2(\sqrt{r}) - {\rm Li}_2(-\sqrt{r})$.

APPENDIX C: C_G COEFFICIENT AT NLO WITH FULL MASS DEPENDENCE

Here we give results for the $C_{\vec{\mu}_G^2}^{\rm NLO}$ coefficient. At NLO we give both color structures.
The C_A color structure coefficient of α_s/π reads

$$\begin{aligned}
C_{\vec{\mu}_G^2}^{{\rm NLO},C_A} = &\frac{1}{108}(1-r)(156-4081r-354r^2-405r^3)\\
&+\frac{1}{9}(6{\rm Li}_2(r)-\pi^2)(1-6r+24r^2-11r^3)\\
&-\frac{(1-r)}{54r}(15+20r-196r^2-292r^3-27r^4)\ln(1-r)\\
&-\frac{1}{54}r(786+972r+131r^2-27r^3)\ln(r) - \frac{2}{9}(1+9r-93r^2+19r^3)\ln(1-r)\ln(r)\\
&+\frac{1}{9}r(9-33r+5r^2)\ln(r)^2\\
&+\frac{8}{3}r^{1/2}\left(1-\frac{11}{3}r\right)\left(4{\rm Li}_2^- - \pi^2 - 2\ln(r)\ln\left(\frac{1+\sqrt{r}}{1-\sqrt{r}}\right)\right).
\end{aligned} \tag{C1}$$

The C_F color structure is

$$
\begin{aligned}
C_{\bar{\mu}_G^2}^{\mathrm{NLO},C_F} = & -\frac{1}{216}(1-r)(321-13747r+5421r^2-3807r^3) \\
& +\frac{1}{18}(6\mathrm{Li}_2(r)-\pi^2)(5+72r-72r^2-88r^3+45r^4) \\
& -\frac{(1-r)}{54r}(12-19r+917r^2-1795r^3+585r^4)\ln(1-r) \\
& +\frac{1}{54}r(1500-330r+2668r^2-585r^3)\ln(r) \\
& +\frac{2}{9}(11+54r-48r^2-94r^3+45r^4)\ln(1-r)\ln(r) \\
& -\frac{1}{18}r(72+60r-112r^2+45r^3)\ln(r)^2 \\
& +\frac{32}{3}\left(1-\frac{4}{3}r\right)r^{1/2}\left(4\mathrm{Li}_2^-\left(\frac{1+\sqrt{r}}{1-\sqrt{r}}\right)-\pi^2-2\ln(r)\ln\left(\frac{1+\sqrt{r}}{1-\sqrt{r}}\right)\right).
\end{aligned}
\tag{C2}
$$

[1] J. Charles *et al.*, Phys. Rev. D **91**, 073007 (2015).
[2] S. Forte *et al.*, arXiv:1505.01279.
[3] J. N. Butler *et al.* (Quark Flavor Physics Working Group Collaboration), arXiv:1311.1076.
[4] A. J. Bevan *et al.* (*BABAR* and Belle Collaborations), Eur. Phys. J. C **74**, 3026 (2014).
[5] T. Kinoshita and A. Sirlin, Phys. Rev. **113**, 1652 (1959).
[6] S. M. Berman, Phys. Rev. **112**, 267 (1958).
[7] T. van Ritbergen and R. G. Stuart, Phys. Rev. Lett. **82**, 488 (1999).
[8] A. A. Pivovarov, Yad. Fiz. **66**, 934 (2003) [Phys. At. Nucl. **66**, 902 (2003)].
[9] J. H. Kuhn, A. I. Onishchenko, A. A. Pivovarov, and O. L. Veretin, Phys. Rev. D **68**, 033018 (2003).
[10] A. A. Petrov and D. V. Zhuridov, Phys. Rev. D **89**, 033005 (2014).
[11] M. A. Shifman and M. B. Voloshin, Sov. J. Nucl. Phys. **41**, 120 (1985).
[12] H. Georgi, Phys. Lett. B **240**, 447 (1990).
[13] M. Neubert, Phys. Rep. **245**, 259 (1994).
[14] A. V. Manohar and M. B. Wise, *Heavy Quark Physics* (Cambridge University Press, Cambridge, England, 2000).
[15] T. Mannel, S. Turczyk, and N. Uraltsev, J. High Energy Phys. 11 (2010) 109.
[16] A. Pak and A. Czarnecki, Phys. Rev. D **78**, 114015 (2008).
[17] S. Biswas and K. Melnikov, J. High Energy Phys. 02 (2010) 089.
[18] T. Becher, H. Boos, and E. Lunghi, J. High Energy Phys. 12 (2007) 062.
[19] A. Alberti, T. Ewerth, P. Gambino, and S. Nandi, Nucl. Phys. **B870**, 16 (2013).
[20] A. Alberti, P. Gambino, and S. Nandi, J. High Energy Phys. 01 (2014) 147.
[21] T. Mannel, A. A. Pivovarov, and D. Rosenthal, Phys. Lett. B **741**, 290 (2015).
[22] A. A. Penin and A. A. Pivovarov, Phys. Lett. B **443**, 264 (1998).
[23] I. I. Y. Bigi, M. A. Shifman, N. G. Uraltsev, and A. I. Vainshtein, Phys. Rev. Lett. **71**, 496 (1993).
[24] T. Mannel, W. Roberts, and Z. Ryzak, Nucl. Phys. **B368**, 204 (1992).
[25] A. V. Manohar, Phys. Rev. D **56**, 230 (1997).
[26] D. Benson, I. I. Bigi, T. Mannel, and N. Uraltsev, Nucl. Phys. **B665**, 367 (2003).
[27] T. van Ritbergen, Phys. Lett. B **454**, 353 (1999).
[28] A. Pak and A. Czarnecki, Phys. Rev. Lett. **100**, 241807 (2008).
[29] K. Melnikov, Phys. Lett. B **666**, 336 (2008).
[30] A. G. Grozin and M. Neubert, Nucl. Phys. **B508**, 311 (1997).
[31] S. Balk, J. G. Korner, and D. Pirjol, Nucl. Phys. **B428**, 499 (1994).
[32] A. V. Manohar and M. B. Wise, Phys. Rev. D **49**, 1310 (1994).
[33] I. I. Y. Bigi, B. Blok, M. A. Shifman, N. G. Uraltsev, and A. I. Vainshtein, arXiv:hep-ph/9212227.
[34] S. Groote, J. G. Korner, and A. A. Pivovarov, Ann. Phys. (Amsterdam) **322**, 2374 (2007); Phys. Lett. B **443**, 269 (1998).
[35] A. C. Hearn, REDUCE User's manual, Version 3.8, http://www.reduce-algebra.com/docs/reduce.pdf.
[36] http://www.wolfram.com/mathematica/.
[37] http://www.feyncalc.org/.
[38] F. V. Tkachov, Phys. Lett. **100B**, 65 (1981); K. G. Chetyrkin and F. V. Tkachov, Nucl. Phys. **B192**, 159 (1981).
[39] R. N. Lee, J. Phys. Conf. Ser. **523**, 012059 (2014).
[40] T. Huber and D. Maitre, Comput. Phys. Commun. **178**, 755 (2008).

[41] Y. Nir, Phys. Lett. B **221**, 184 (1989).
[42] I. Allison *et al.* (HPQCD Collaboration), Phys. Rev. D **78**, 054513 (2008).
[43] J. Beringer *et al.* (Particle Data Group Collaboration), Phys. Rev. D **86**, 010001 (2012).
[44] N. V. Krasnikov and A. A. Pivovarov, Yad. Fiz. **64**, 1576 (2001) [Phys. At. Nucl. **64**, 1500 (2001)]; Mod. Phys. Lett. A **11**, 835 (1996).
[45] A. A. Penin and A. A. Pivovarov, Phys. Lett. B **435**, 413 (1998).
[46] I. I. Y. Bigi, A. G. Grozin, M. A. Shifman, N. G. Uraltsev, and A. I. Vainshtein, Phys. Lett. B **339**, 160 (1994).
[47] J. G. Korner, F. Krajewski, and A. A. Pivovarov, Phys. Rev. D **63**, 036001 (2000).
[48] A. F. Falk, M. E. Luke, and M. J. Savage, Phys. Rev. D **53**, 2491 (1996).
[49] A. Alberti, P. Gambino, K. J. Healey, and S. Nandi, Phys. Rev. Lett. **114**, 061802 (2015).
[50] P. Gambino and C. Schwanda, Phys. Rev. D **89**, 014022 (2014).